

Symmetry-Resolved Absorption Spectra of Vibrationally Excited CO₂ Molecules

T. Tanaka,¹ C. Makochekanwa,^{1,2} H. Tanaka,¹ M. Kitajima,¹ M. Hoshino,³ Y. Tamenori,⁴ E. Kukkk,^{5,6} X. J. Liu,⁵
G. Prümper,⁵ and K. Ueda^{5,*}

¹Department of Physics, Sophia University, Tokyo 102-8554, Japan

²Graduate School of Sciences, Kyushu University, Fukuoka 812-8581, Japan

³Atomic Physics Laboratory, RIKEN, Wako, Saitama 351-0198, Japan

⁴Japan Synchrotron Radiation Research Institute, Sayo-gun, Hyogo 679-5198, Japan

⁵Institute of Multidisciplinary Research for Advanced Materials, Tohoku University, Sendai 980-8577, Japan

⁶Department of Physics, Materials Science, University of Turku, FIN-20014, Turku, Finland

(Received 10 March 2005; published 9 November 2005)

Symmetry-resolved x-ray absorption spectroscopy has been first carried out on high-temperature molecules. From the angle-resolved ion yield spectra of CO₂ both at room temperature and at 430 °C, symmetry-resolved absorption profiles of the C $1s^{-1}2\pi_u$ and O $1s^{-1}2\pi_u$ resonances have been extracted for the vibrational ground state molecules and bending-vibration excited ones. The profiles change dramatically between them, and the Renner-Teller effect becomes more evident for the vibrationally excited molecules. The effects of the multimode vibronic coupling are suggested for the O $1s^{-1}2\pi_u$ and O $1s^{-1}3s\sigma_g$ resonances.

DOI: 10.1103/PhysRevLett.95.203002

PACS numbers: 33.20.-t, 33.70.-w

The carbon dioxide molecules CO₂, besides being a greenhouse gas, are very important from an astrophysical point of view. CO₂ constitutes about 95% of Venus's atmosphere, the average surface of which is ~460 °C. At such temperatures, the molecules are partially vibrationally excited and these molecular vibrations must be taken into account for proper atmospheric modeling [1]. However, there are only a few studies of vibrationally excited *hot* molecules in the region of the extreme vacuum ultraviolet absorption spectroscopy [2] and in the area of low-energy electron collisions [3]. To our knowledge, no x-ray absorption study has been reported so far on any hot molecules. This Letter reports the first x-ray absorption study on the hot CO₂ molecules.

The CO₂ molecules are also the most suitable and simplest system to study the interaction between nuclear and electronic motions, often called *vibronic interaction*. The vibronic interaction has been one of the key issues in molecular physics since its effects are widely spread, even to solid state physics and material science [4]. Here we cite only some works directly related to the present work on C $1s$ and O $1s$ core excitations of CO₂ [5–14]. The stable geometry of CO₂ in the ground state is linear and belongs to the $D_{\infty h}$ point group. A promotion of the $2\sigma_g$ (C $1s$) core electron to the lowest unoccupied molecular orbital $2\pi_u$ leads to the doubly degenerate Π_u state that splits into two as a consequence of vibronic coupling via the bending vibration ν_2 , referred to as the Renner-Teller effect [5,8,10,12]. Removing one O $1s$ core electron, or promoting it to a Rydberg orbital, leads to symmetry lowering as a consequence of vibronic coupling, referred to as the pseudo-Jahn-Teller coupling, which mixes the nearly degenerate states $1\sigma_g^{-1}$ and $1\sigma_u^{-1}$ via the antisymmetric stretching vibration ν_3 [6,7,13]. In the present work, we

demonstrate that the vibrational excitation of the CO₂ molecules dramatically affects the x-ray absorption profile because of the enhanced vibronic coupling effects.

The experimental technique we employ here is angle-resolved ion yield spectroscopy, whereby fragment ions are detected parallel and perpendicular to the light polarization vector E , hereafter referred to as the 0° and 90° spectra, respectively. This technique is often called *symmetry-resolved* absorption spectroscopy [15] based on the fact that the direction of ion ejection directly reflects the axis of the linear molecule at the time of photoabsorption (axial-recoil approximation) [16,17]. This means that fragment ions from the $\Sigma \rightarrow \Sigma$ and $\Sigma \rightarrow \Pi$ transitions are detected preferentially in the 0° and 90° directions, respectively. It has been demonstrated that this technique is also very powerful in studying vibronic coupling effects in linear molecules [8]. Using this technique, Yoshida *et al.* characterized the splitting of the C $1s^{-1}2\pi_u$ state into Renner-Teller states, i.e., the bent A_1 and linear B_1 states [12].

The experiment has been carried out at the beam line 27SU at SPring-8 in Japan, using a high-resolution soft x-ray monochromator [18]. Two identical ion detectors, to each of which a retarding potential of 6 V is applied, are mounted at 0° and 90° with respect to the E vector [11]. The angle-resolved measurements of the ion yields using these detectors have been carried out at room temperature and at 430 °C. The high-temperature sample gas was produced by the resistively heated molecular beam source. A 4π -sr ion detector is placed 250 mm away and used to measure the total ion yield (TIY) simultaneously with the angle-resolved ion yields. Note, however, that the TIY spectra always represent room-temperature spectra, since we use the residual gas in the vacuum chamber for the TIY measurements. The pressure in the vacuum chamber was

$\sim 8 \times 10^{-4}$ Pa during the measurements. The photon bandwidth of the monochromator was set to 38 meV for the C $1s$ excitation region and to 50 meV for the O $1s$ excitation region. The photon energy scales were calibrated using the peak energies, 290.77 [19] and 535.4 eV [5] for the C $1s^{-1}2\pi_u$ and O $1s^{-1}2\pi_u$ resonances, respectively.

In each of the spectra measured at room temperature and at 430 °C, the baseline, comprising contributions from the valence ionization and ionization by the second order and assumed more or less constant, was first subtracted. Then it was assumed that the total number of populations was conserved between the ground state and the combined vibrationally excited states. According to the above assumption, the combined spectra $I = I(0) + 2 \times I(90)$ were normalized to the same area for both room- and high-temperature measurements, so that the change in the density of the molecules in the source volume by the temperature difference was compensated. The normalization coefficients thus obtained were then applied to the original 0° and 90° spectra, which are presented in Figs. 1 and 2, for the C $1s^{-1}2\pi_u$ and O $1s^{-1}2\pi_u$ resonances, respectively. The simultaneously measured TIY spectra are also included for reference. The room-temperature spectra are in good agreement with previous measurements recorded with similar resolutions [9–12].

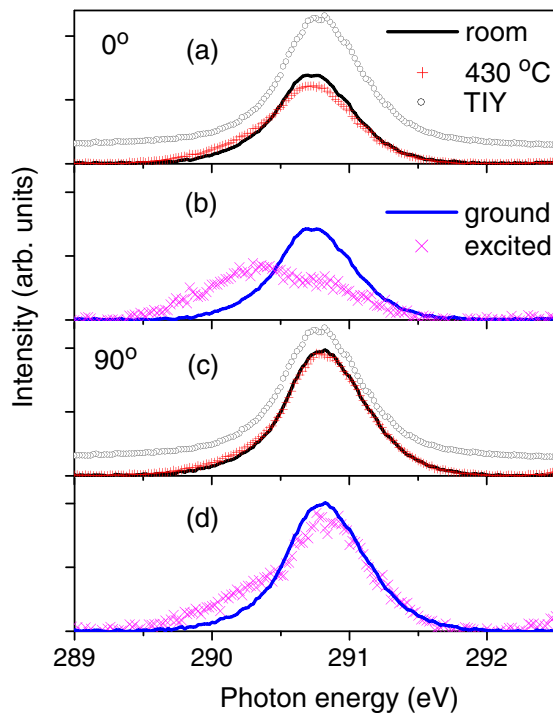


FIG. 1 (color online). Absorption spectra in the CO_2 C $1s^{-1}2\pi_u$ excitation region: (a) 0° spectra measured at room temperature and at 430 °C and the TIY spectra; (b) extracted ground and vibrationally excited state 0° spectra. (c),(d) 90° spectra with same descriptions as (a) and (b), respectively.

All measured ion yield spectra can be taken as comprising of two “pure” photoabsorption spectra—one from the ensemble of molecules in the vibrational *ground* state and the other in the vibrationally *excited* state. The population of these ensembles is given by the Boltzmann distribution at a given temperature. In our case of CO_2 , the first vibrationally excited state, at 83 meV above the ground state, is due to a bending vibration [20]. The Boltzmann distribution probabilities of 74.6% and 95.6% were assumed for the ground state at 430 °C and at room temperature, respectively. Solving the two simultaneous equations derived from these probabilities, we obtain the following relationships between the measured spectra I_{hot} and I_{room} and the pure spectra I_{ground} and I_{excited} :

$$I_{\text{excited}} = 4.545(I_{\text{hot}} - 0.780I_{\text{room}}), \quad (1)$$

$$I_{\text{ground}} = 0.211(5.773I_{\text{room}} - I_{\text{hot}}). \quad (2)$$

At these temperatures, the probability of exciting thermally two quanta of the bending mode is very small, being only $\sim 4.8\%$ for $\nu_2 = 2$, and, thus, we will regard I_{excited} as a spectrum from the molecules in the first vibrationally excited state. Based on Eqs. (1) and (2), the excited and ground state angle-resolved absorption spectra were derived from the measured room-temperature and 430 °C spectra and for the two detection angles of 0° and 90° . These results are shown in Figs. 1 and 2, for the C $1s^{-1}2\pi_u$ and O $1s^{-1}2\pi_u$ resonances, respectively.

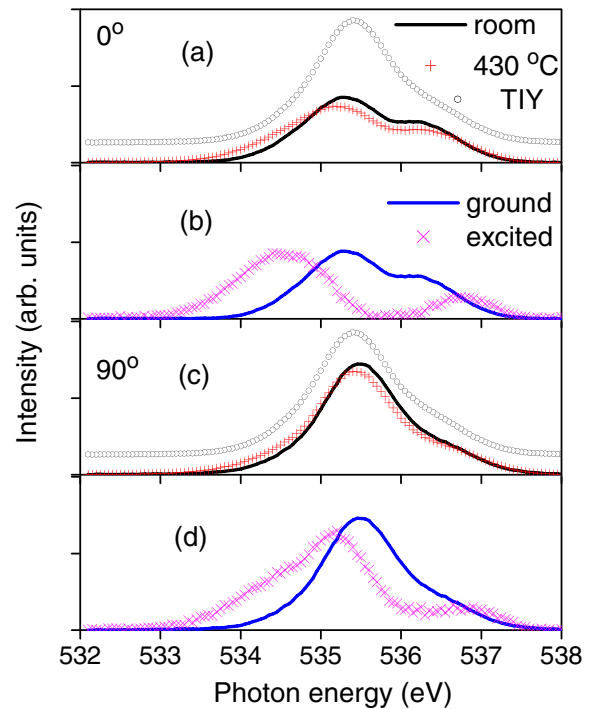


FIG. 2 (color online). Absorption spectra in the CO_2 O $1s^{-1}2\pi_u$ excitation region. See the caption of Fig. 1 for details.

First we consider the $C 1s^{-1}2\pi_u$ resonance. As mentioned earlier, the $C 1s^{-1}2\pi_u$ photoabsorption takes place preferentially for the molecules whose axes are aligned in the direction at 90° to E . Therefore, in the limit of the axial-recoil approximation [15–17], energetic fragments from the *linear* CO_2 molecules can be detected only at the 90° angle. The $C 1s^{-1}2\pi_u$ state, however, splits into two due to the Renner-Teller effect, the lower-energy branch being the bent A_1 state and the higher-energy branch the linear B_1 state [5,8,10,12]. The formation of the bent geometry in the core-excited state violates the axial-recoil approximation. The detection of fragment ions by the 0° detector reflects the bending motion of the molecules in the bent A_1 state [8,12].

We first compare the ground and excited state 0° spectra in Fig. 1(b). These spectra include only the excitation to the bent $C 1s^{-1}2\pi_u A_1$ state. The band profile of the excited state spectrum is much broader and its peak energy is shifted to lower photon energies by ~ 0.4 eV, in comparison to the ground state spectrum. The broadening and shift can be understood with the help of the potential curve for the A_1 state as a function of the O-C-O angle. The potential curves in Fig. 3 are generated from the results given in Ref. [14]. The ground electronic state of CO_2 is linear, and the nuclear wave function of the ground state has its maximum at the O-C-O angle of 180° . Because of the Franck-Condon principle, the photoabsorption from the vibrational ground state to the bent A_1 state preferably populates vibronic states with energies close to the top of the central maximum, since their wave functions also have maxima near the 180° O-C-O angle. On the other hand, the

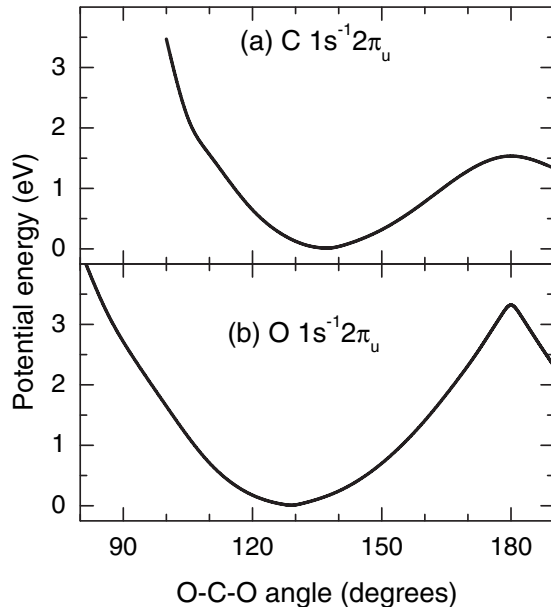


FIG. 3. Potential energy curves for the $C 1s^{-1}2\pi_u A_1$ and $O 1s^{-1}2\pi_u A_1$ states as functions of the O-C-O angle, calculated using the Hartree-Fock approximation within the equivalent core model. The curves are generated from the results given in Ref. [14].

nuclear wave function for the first excited level of the bending mode in the electronic ground state has a node at the 180° O-C-O angle, and the probability density maxima are shifted away from 180° . By projecting these maxima onto the potential energy curve of the excited state, i.e., in the reflection approximation, it can be seen that the photoabsorption now preferentially reaches the vibronic states with energies lower than the local maximum of the A_1 state, where the slope of the potential curve is steeper than at 180° . Note that the width of the vibrational envelope is determined by the rate of change slope of the potential curve, i.e., the slower the change of slope, the narrower the feature, and vice versa. Thus, already this qualitative argument predicts a broadening and a shift towards lower photon energies of the vibrational envelope in the photoabsorption spectrum for the vibrationally excited state, compared to the ground state spectrum.

Contrary to the 0° spectra, the 90° spectra in Fig. 1(d) include both contributions from the bent A_1 and linear B_1 states. The excited state spectrum has a longer low-energy tail than the ground state spectrum. This low-energy tail mimics the low-energy part of the 0° spectra and, thus, can be attributed to the contribution from the bent A_1 state. The main peak and the high-energy tail, on the other hand, can be attributed to the linear B_1 state. The peak energy and the profile of the higher-energy tail do not change between the excited and ground state spectra, suggesting that the potential curves along the bending motion for the ground and B_1 state are parallel. See the discussions above (and below) on the relationship between the spectrum energy position and profile and the potential curve.

Now we consider the $O 1s^{-1}2\pi_u$ resonance spectra. The ground and excited state 0° spectra in Fig. 2(b) do not include the excitation to the linear $O 1s^{-1}2\pi_u B_1$ state. Thus, the main peak is attributed to the photoabsorption to the bent $O 1s^{-1}2\pi_u A_1$ state. The peak energy of the A_1 band in the excited state spectrum is shifted towards lower photon energies by ~ 0.8 eV relative to that in the ground state spectrum. This shift is 2 times larger than that in the $C 1s^{-1}2\pi_u$ resonance spectra in Fig. 1. The broadening of the A_1 band in the excited state spectrum relative to that in the ground state spectrum is not as dramatic as that in the $C 1s^{-1}2\pi_u$ resonance spectra in Fig. 1. These differences can be explained with reference to the difference between the potential energy curves between the $C 1s^{-1}2\pi_u A_1$ and $O 1s^{-1}2\pi_u A_1$ states illustrated in Fig. 3. The photoabsorption from the ground and excited states to the A_1 state reaches the vibronic states with energies at the O-C-O angles close to $\sim 180^\circ$ and at smaller O-C-O angles, respectively. The potential curve of the $O 1s^{-1}2\pi_u A_1$ state has a cusp structure at 180° sharper than that of the $C 1s^{-1}2\pi_u A_1$ state. As a result, the energy shift in the absorption peak in the excited state spectrum relative to the ground state spectrum is much larger in $O 1s^{-1}2\pi_u$ than in $C 1s^{-1}2\pi_u$. However, the slope of the potential curve does

not change much at the O-C-O angles concerned and, thus, the similarity in width between the vibrational envelope of the ground state and that of the excited state spectra. These features contrast with those for the C $1s^{-1}2\pi_u$ resonance, where the width of the vibrational envelope changes drastically depending on whether the initial state is vibrationally excited or not. The shoulder at the higher-energy side, above 535.9 eV in the ground state spectrum, is attributed to the photoabsorption to the O $1s\sigma_u^{-1}3s\sigma_g\Sigma_u$ state. In the excited state spectrum, the $3s$ band stands out clearly separated from the A_1 band.

The ground and excited state 90° spectra in Fig. 2(d) include excitations to both the O $1s^{-1}2\pi_u B_1$ linear and A_1 bent states as well as the O $1s\sigma_u^{-1}3s\sigma_g\Sigma_u^+$ state. As discussed for the C $1s^{-1}2\pi_u A_1$ and B_1 states, the B_1 state is located at higher energies than the A_1 state. Thus, the energy of the main peak in the 90° ground state spectrum is slightly higher than that in the ground state 0° spectrum. In the excited state 90° spectrum, the three components become more clearly visible. The main peak at 535.1 eV can be attributed to the linear B_1 state. Both the low-energy tail below 534.5 eV and the high-energy broad peak above 536 eV mimic the excited state 0° spectrum, the low-energy tail being attributed to the bent A_1 state and the high-energy broad peak to the $3s\sigma_g$ band. The $3s\sigma_g$ band appears in the 90° spectrum because of the vibronic coupling between the O $1s\sigma_g^{-1}2\pi_u\Pi_u$ and O $1s\sigma_g^{-1}3s\sigma_g\Sigma_g$ via the bending vibration with π_u symmetry, i.e., the so-called pseudo-Jahn-Teller coupling. The $3s$ band in the 90° spectrum is thus assigned to the O $1s\sigma_g^{-1}3s\sigma_g\Sigma_g \otimes \pi_u$ (odd number of vibrations) Π_u vibronic state.

There are a couple of points which cannot be explained within the framework of only the single-mode vibronic coupling outlined so far. First, the peak energy in the excited 90° spectrum, which is attributed to the O $1s^{-1}2\pi_u B_1$ band, is shifted down by ~ 0.4 eV in comparison to that in the ground state 0° spectrum. This contrasts with the fact that the corresponding peak energy for the C $1s^{-1}2\pi_u B_1$ band does not change when the initial state is vibrationally excited. Second, the peak energy of the $3s$ band in the excited state spectrum is shifted up in comparison to that in the ground state spectrum. In case of the O $1s$ excited states, both Renner-Teller coupling via the bending vibration ν_2 and pseudo-Jahn-Teller coupling via the antisymmetric stretching vibration ν_3 play a significant role. Thus, multimode couplings which involve these two vibrational modes are also expected. A theoretical study which includes multimode vibronic couplings seems to be indispensable to fully understand the O $1s$ absorption spectra of the vibrationally excited CO₂ molecules. For details on these multimode vibronic couplings and their effects, see Ref. [21], and references therein.

In conclusion, we have for the first time succeeded in obtaining symmetry-resolved x-ray absorption spectra of the vibrationally excited CO₂ molecules in the regions of the C $1s^{-1}2\pi_u$ and O $1s^{-1}2\pi_u$ resonances. The enhanced Renner-Teller effect has been observed for both resonances and qualitatively explained referring to the relevant potential curves. Some observations for the O $1s$ excitation suggest the effects of multimode vibronic couplings and remain a challenge for further theoretical study for the complete elucidation.

The experiment was carried out with approval of the SPring-8 program review committee and supported in part by Grants-in-Aid for Scientific Research from the Japan Society for the Promotion of Science (JSPS). C.M. is grateful to the JSPS for financial support. E.K. is also grateful to Tohoku University for the hospitality and financial support. The authors also acknowledge the Sophia University Techno Center Staff for their help in making the heating furnace.

*Corresponding author.

Electronic address: ueda@tagen.tohoku.ac.jp

- [1] See <http://www.adlerplanetarium.org/learn/planets/venus/>.
- [2] C. Y. R. Wu, D. L. Judge, and T. Matsui, *J. Electron Spectrosc. Relat. Phenom.* **144**, 123 (2005).
- [3] J. Ferch *et al.*, *Phys. Rev. A* **40**, 5407 (1989), and references therein.
- [4] I. B. Bersuker and V. Z. Polinger, *Vibronic Interactions in Molecules and Crystals* (Springer, Berlin, 1989).
- [5] G. R. Wight and C. E. Brion, *J. Electron Spectrosc. Relat. Phenom.* **3**, 191 (1974).
- [6] W. Domcke and L. S. Cederbaum, *Chem. Phys.* **25**, 189 (1977).
- [7] A. Kivimäki *et al.*, *Phys. Rev. Lett.* **79**, 998 (1997).
- [8] J. Adachi *et al.*, *J. Chem. Phys.* **107**, 4919 (1997).
- [9] K. C. Prince *et al.*, *J. Phys. B* **32**, 2551 (1999).
- [10] E. Kukk *et al.*, *Phys. Rev. A* **62**, 032708 (2000).
- [11] N. Saito *et al.*, *Phys. Rev. A* **62**, 042503 (2000).
- [12] H. Yoshida *et al.*, *Phys. Rev. Lett.* **88**, 083001 (2002).
- [13] K. Okada *et al.*, *Phys. Rev. A* **66**, 032503 (2002).
- [14] N. Saito *et al.*, *J. Electron Spectrosc. Relat. Phenom.* **141**, 183 (2004).
- [15] E. Shigemasa *et al.*, *Phys. Rev. A* **45**, 2915 (1992).
- [16] R. N. Zare, *Mol. Photochem.* **4**, 1 (1972).
- [17] G. E. Busch and K. R. Wilson, *J. Chem. Phys.* **56**, 3638 (1972).
- [18] H. Ohashi *et al.*, *Nucl. Instrum. Methods Phys. Res., Sect. A* **467-468**, 533 (2001).
- [19] M. Tronc, G. C. King, and F. R. Read, *J. Phys. B* **12**, 137 (1979).
- [20] Y. Ma *et al.*, *Phys. Rev. A* **44**, 1848 (1991).
- [21] K. Ueda *et al.*, *Phys. Rev. Lett.* **85**, 3129 (2000).